

# Breaking of the $\sqrt{N}$ limit in least squares resolution and the dirty-lucky model

Gregorio Landi<sup>a\*</sup>, Giovanni E. Landi<sup>b</sup>

<sup>a</sup> Dipartimento di Fisica e Astronomia, Università di Firenze and INFN  
Largo E. Fermi 2 (Arcetri) 50125, Firenze, Italy

<sup>b</sup> ArchonVR S.a.g.l.,  
Via Cisieri 3, 6900 Lugano, Switzerland.

December 15, 2024

## Abstract

Very simple gaussian simulations show a fitting result with a linear growth in the number  $N$  of detecting layers. This rule is well beyond the well known rule as  $\sqrt{N}$  typical of a standard fit. The effect is obtained with the appropriate use of the variance of each hit (measurement). The model reconstructs straight tracks in a tracker with  $N$  parallel detecting layers with very simple statistical errors. The results of this model are compared with realistic simulations of silicon microstrip detectors. These realistic simulations suggest an easy method to select essential parameters for the fits: the dirty-lucky model. Preliminary results of the dirty-lucky model show excellent reproduction of the simulations and the linear growth.

Keywords: Least squares method, Resolution, Position Reconstruction, Microstrip Detectors,  
PACS: 07.05.Kf, 06.30.Bp, 42.30.Sy

## 1 Introduction

The new fitting method, described in refs. [1, 2], is producing interesting and unexpected results. One of those achievements, shown in ref. [2], displays a linear growth of the momentum resolution with the number  $N$  of detecting layers. This result is strikingly different from the textbook result that easily demonstrates a growth in resolution as  $\sqrt{N}$  in least squares fits. Even if  $\sqrt{N}$  refers to the fit of a constant, we will recall this type of rule even for other fitted parameters where the rule is not so simple. To illustrate with further details the generality of our linear growth, we study the fit of the direction of a minimum ionizing particle (MIP) crossing a simpler tracker. The tracker model is formed by  $N$  parallel detecting layers of identical technology, without magnetic field and exposed to a well collimated beam of high momentum MIPs (to neglect the multiple scattering). To fix the ideas we suppose silicon microstrip detecting layers, but, this one is not an essential condition. The simplicity of the simulation gives a direct explanation of the results of our complete fitting method, that is extremely more complex than any other discussed in literature. Dedicated mathematical tools have been developed in refs. [1, 2] to extract details of the detectors to insert in the fit. A more meditate analysis of those details allows the discovery of essential simplifications of our approach.

---

\*Corresponding author. Gregorio.Landi@fi.infn.it

As a preliminary step, let us review the assumptions contained in the standard least squares method. The most frequent one assumes that all the measurements have identical variance. This condition is defined in statistics as homoscedasticity. It introduces a drastic shortcut in the equations that become independent from the data variances. The opposite of homoscedasticity is indicated as heteroscedasticity. In this case the identity of the variances is abandoned. The equations for the least squares consider this case, but, in real applications, heteroscedasticity is completely neglected. It is weakly considered in track fitting if the detector property/technology is changed. In this case, a single effective variance [3] for all the hits in the layer is used in the fit. The simplification introduced by identical variances can not hide its nonphysical content. In fact, homoscedasticity, to be truly realized, requires some kind of hard symmetry. This symmetry is very improbable in a complicated world, full of small or large variations in detector quality, local physical anisotropy (noisy strips), anisotropy of the reconstruction algorithms, etc.. Thus, the large majority of physical data are surely heteroscedastic, but they are handled as homoscedastic. In the present generation of trackers, these simplifications and many others are relevant to reconstruct the enormous number of tracks produced. But, the loss of resolution of the standard methods could be carefully scrutinized, especially if very fast suboptimal tools can be defined.

Here a simple gaussian model will be tested to illustrate the set up of the linear growth in  $N$  due to a special form of heteroscedasticity. This gaussian model is compared with a more realistic model. We limit the realistic simulations to a single detector type, very similar to silicon strip detectors largely used in running experiments. A preliminary introduction of a fast suboptimal tool (the dirty-lucky model) will be discussed and compared with realistic simulations. We limit our discussion to the recipes to obtain these results, the mathematical details will be published elsewhere.

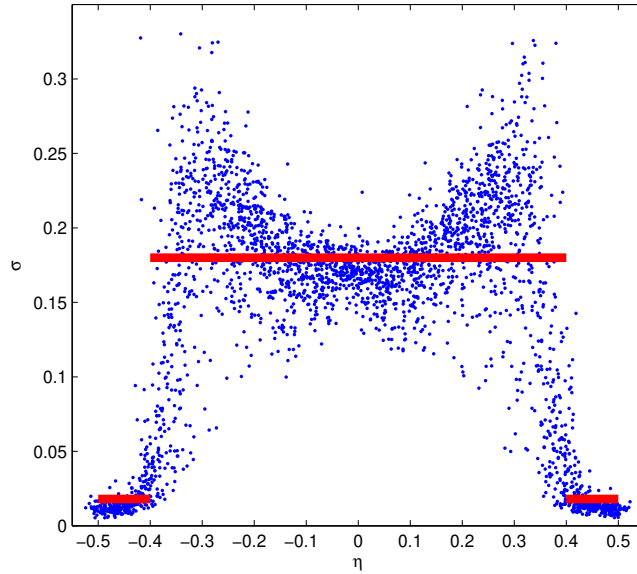


Figure 1: The red lines are the values of  $\sigma$  of the gaussian model. The blue dots are the effective  $\sigma$ 's of the realistic model. The dimensions are in strip width ( $63\mu\text{m}$ ). The  $\eta$ -algorithm gives the hit positions.

## 2 A simple gaussian model

The model we explore is a gaussian model with two different standard deviations ( $\sigma$ ), one of 0.18 with a probability of 80 % and the other of 0.018 with a probability of 20%: hard symmetry with a small "spontaneous" symmetry breaking. The relation of this model with the full realistic model of silicon micro-strips is illustrated in fig. 1. It represents a drastic simplification of the models of refs. [1, 2].

Few lines of MATLAB [4] code suffice to produce this simulation, and they could be a viable substitute of long mathematical developments. A large number of gaussian random numbers, with zero average and unity standard deviation, are generated (with the MATLAB `randn` function). Each one is multiplied by one of the two standard deviations (0.18, 0.018) with the given relative probability (80%, 20%). The data are scrambled and recollected to simulate a set of parallel tracks crossing few detector layers. Each track hits the  $N$  detector layers in uncorrelated random points (binomial probability rule). The detector layers are supposed parallel, but the strips have slight rotations as in real trackers. This is the worst case, a perfect alignment would amplify this effect. Due to the translation invariance, the tracks can be expressed by a single equation  $x_i = \beta + \gamma y_i$  with  $\beta = 0$  and  $\gamma = 0$  for the orthogonal incidence of the beam ( $\beta$  is the impact point of the track,  $\gamma$  the direction and  $y_i$  the positions of the detector layers). The distributions of  $\gamma_f$ , given by the fit, are the object of our study. This parameter is a constant in a standard test beam (a Dirac- $\delta$  function will be assumed as  $\gamma$ -distribution) and its fitted values can give indications of the heteroscedasticity of the detector. The distance of first and the last detector layer is the length of the PAMELA [10] tracker (445 mm), but this is not essential. Other "detector layers" are inserted symmetrically in this length. Two different least squares fits are compared. One uses identical  $\sigma$  of each hit (we call this standard fit). The other fit applies the appropriate  $\sigma$ -values to each hit. This second fit shows the linear growth. We generate 150000 tracks for each configuration. The results are reported in fig. 2 as (empirical) probability density functions of  $\gamma_f$ . The parameter  $\gamma_f$  is the tangent of a small angle, a pure small number. To give a scale to the plots of  $\gamma_f$ , we could identify the tangent with its argument and consider the horizontal scale in radians (rad) and the vertical scale as  $\text{rad}^{-1}$ . We will neglect these details in the plots.

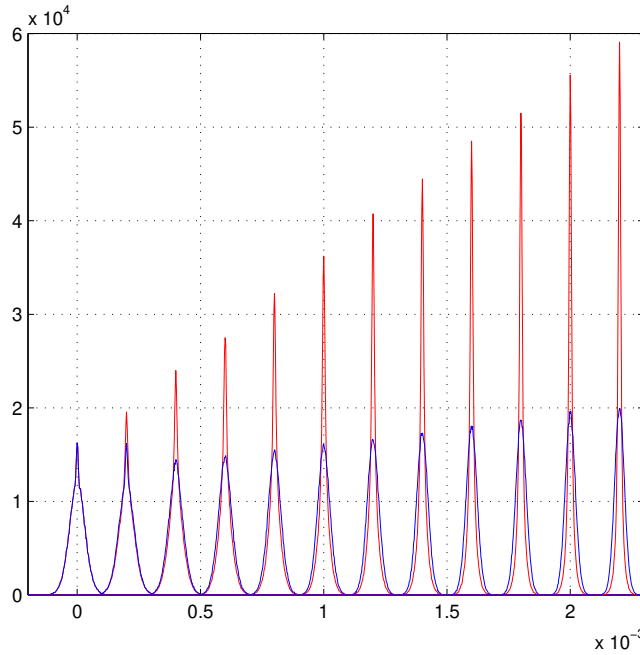


Figure 2: The two gaussian models. The blue distributions of  $\gamma_f$  do not account the  $\sigma$ -values. The linear growth is evident in the red distributions of  $\gamma_f$ . The first distribution is centered on zero, the others are shifted by  $N-2$  identical steps.

All these distributions are centered on the zero, but in this way the plot is unreadable. Thus we have to shift the distributions. The first distribution is centered in zero, as it must be, and the tracker has only two layers. The others with three, four, etc. up to thirteen layers are shifted by  $N - 2$  identical steps to show better the increase. Heteroscedasticity influences the first two distributions (two and three layers) even in the standard fit, in fact if the two hits have a narrow (gaussian) position distributions (small  $\sigma$ ) the  $\gamma_f$

of the fitted tracks is forced to be contained in a narrow distribution. It is curious that to reach the height of these two distributions many other layers must be added (are they useless?). We will consider the height of each distribution as an evaluation of the resolution of the corresponding fit. Actually, the most common distributions have the maximum proportional to the inverse of the full-width-at-half-maximum (FWHM). The FWHM is often considered a measure of the mean error for non gaussian distributions and its inverse is the resolution. If the detector layers are slightly different (as usual) the linear growth will show small distortions due to these differences.

An approximate linear growth can be extracted even from the standard least squares, as illustrated in fig. 3.

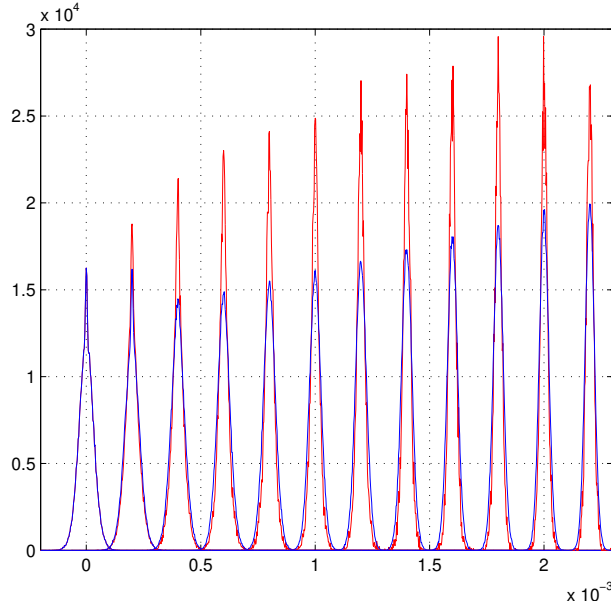


Figure 3: The gaussian model. Extraction of an approximate linear growth from the standard least squares with the selection of low  $\chi^2$ -values.

In fact, for a pure homoscedastic gaussian model, it is a basic demonstration that the fitted parameters are independent random variables (easily verified in these simulations with the elimination of the symmetry breaking). Thus, the presence of a small heteroscedasticity destroys this independence and tends to couple the probability distribution of  $\gamma_f$  with the values of  $\sum_i (x_i - \beta_f - \gamma_f y_i)^2$  for each track (often called  $\chi^2$  [5] as we will do in the following). The parameters  $\beta_f$  and  $\gamma_f$  are those obtained from the least squares fit for that track. Among the lowest values of the  $\chi^2$ , it is more frequent to find good  $\gamma_f$ -values. The gaussian model shows a partial linear increase of the  $\gamma$  distributions selected with  $\chi^2$ . We used the following empirical equation  $\chi^2 < 0.08(N/13)^2$  to account for the  $\chi^2$  increase with N. Figure 3 illustrates this selection, and this violation can be an independent test of heteroscedasticity in addition to those described in the following.

### 3 The schematic model

Similar results can be obtained from our schematic model. This realistic model is called schematic to maintain a consistency with refs. [1, 2]. There, we used this model as a first approximation of the complete model, and as the starting point for the maximum likelihood search. The quality of the fit produced by the schematic model is not far from the complete model, the main differences are in the ability of the complete model to find good results even in presence of the worst hits called *outliers*. The

calculations of the effective variance of each hit is very time consuming, but after an initial (large) set of  $\sigma$  is obtained, the others can be quickly produced with interpolations (high precisions are inessential). Figure 1 shows a subset of effective  $\sigma$  for this type of micro-strip detectors. An interesting aspect of this scatter-plot is the very low values of  $\sigma$  at the strip borders. The positioning algorithm is the  $\eta$ -algorithm of ref. [6]. This algorithm is essential to eliminate the large systematic errors of the two strip center of gravity (COG<sub>2</sub>). The forms of those systematic errors were analytically described in ref. [7], many years later than their full corrections. References [8, 9] added further refinements to the  $\eta$ -algorithm and extended it to any type of center of gravity (COG) algorithm.

A sketchy abstract of the algorithm is reported at pag. 8 of ref. [2]. We underline that the results, shown in the following, are impossible without the  $\eta$ -algorithm. For example, any type of COG algorithms is completely blind to this refined approach. It is uncertain that the statistics has any relation with least squares fits based on COG positioning algorithms. We proved in ref. [2] that the elimination of any random noise (the statistics) does not modify the probability distributions of the fit products based on the COG<sub>2</sub> positions. Instead, the distributions of the fit results based on the  $\eta$ -algorithm rapidly converge toward Dirac- $\delta$  functions as it must be.

Again, our aim will be the fit of straight tracks of equation  $x_i = \beta + \gamma y_i$  with  $\beta = 0$  and  $\gamma = 0$  incident orthogonally to a set of detector layers. The properties of the simulated hits are modeled as far as possible on test-beam data [10], as discussed in ref. [1]. Even now, we compare the  $\gamma_f$  distributions given by two types of least squares. One fit uses the different  $\sigma$  (the blue dots) of the scatter plot of fig. 1 for the hit, and the standard least squares that assumes identical variances for the hits. Figure 4 shows these results.

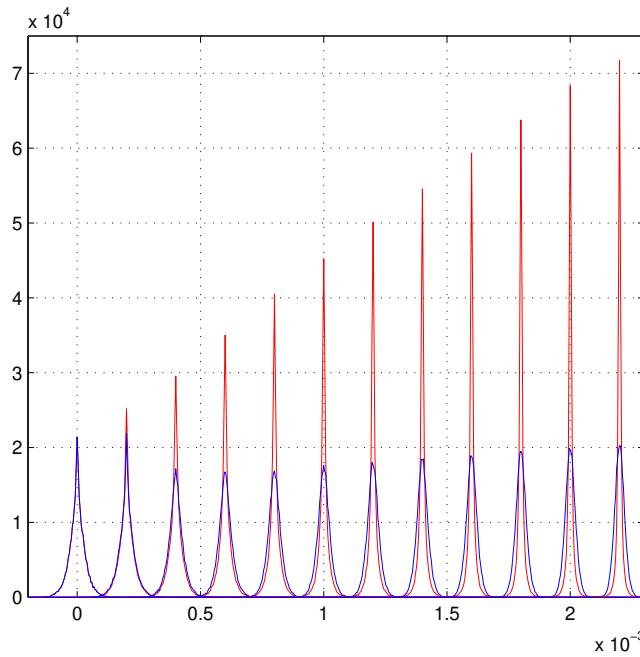


Figure 4: Schematic model. The blue  $\gamma_f$  distributions are the standard least squares fits. The red  $\gamma_f$  distributions show the linear growth and are produced with the effective  $\sigma$  for each hit

## 4 The dirty-lucky model

During the review of ref. [2] one of the three referees of the paper asked us few details about an asymmetry present in figure#1 of ref. [2]. Given our orthogonal incidence, it seems reasonable to expect a

symmetry. Even if this appears a simple demand, we had no real idea/demonstration of the origin of the details in those plots, apart the long list of equations required to arrive to them. In ref. [1] we inserted a very intuitive explanation of the strong similarity of the our scatter plots with the COG<sub>2</sub> histograms of the original data given by the test beam of ref. [10]. Our preliminary analysis did not find any simple relation (scaling factors) able to reproduce the plots. The cut selection we used in the definition of the effective variances (eq.11 of ref. [2]) were essentially based on an aesthetical criterion. We considered relevant the reproduction of parts of the gaussian features when they were present. Essentially we tuned the cuts on a small subset of excellent hits to seek a comparison with our complete probability distributions. The scatter plots of ref. [1] were produced for the first time just for their insertion in the publication. However, once we discarded the possibility of a casual matching, a reasonable explanation could be found of this coincidence. Thus, the referee observation triggers a more accurate analysis of the argument. The use of the equations of ref. [2] allow the construction a very approximate (dirty) demonstration of the consistency of the shapes of our scatter plots. A by-product of that is a geometrical evidence of a resolution increase at the strip borders, just the origin of the linear growth. All the details of this preliminary demonstration will be published elsewhere, with the hope to obtain something better. For example, a simple scaling must be ruled out, non-linear terms are required. Figure 5 illustrates this very rough matching of the  $\sigma$  scatter plot and the COG<sub>2</sub> histogram. The  $\sigma$ -values are scaled to produce an approximate overlap with the COG<sub>2</sub> histogram.

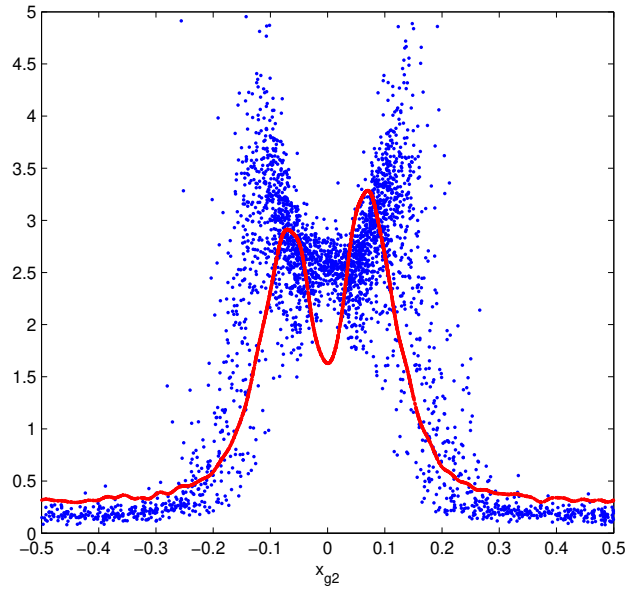


Figure 5: Scatter plot of the effective  $\sigma$  as function of the COG<sub>2</sub> ( $x_{g2}$ ) scaled to reach an approximate overlap with the COG<sub>2</sub> histogram (red dots) as given by the  $\eta$ -algorithm

Here we recall the intuitive explanation of ref. [1]. The effective  $\sigma$  estimates the ranges of the possible impact values converging to the same COG<sub>2</sub> value. Hence, larger  $\sigma$  gives higher COG<sub>2</sub> probability and lower  $\sigma$  gives lower COG<sub>2</sub> probability. Inverting this statement, it looks reasonable that hits with the lower COG<sub>2</sub> probability have lower effective  $\sigma$  and hits in the higher COG<sub>2</sub> probability have higher effective  $\sigma$ . If these assumptions would be successful we have a very economic strategy to implement heteroscedasticity in the track fitting with pieces of information that were well hidden just in front of us. But, without the hints of the scatter plots of ref. [1], they could remain hidden. The COG<sub>2</sub> probabilities are very easy to obtain from the corresponding histograms or as a by product of the  $\eta$ -algorithm [8]. Further details are required, the scaling factors to render compatible the COG<sub>2</sub> histograms and effective  $\sigma$  scatter plots. At least these scaling factors must be calculated. But, for identical detectors, as in our

case, an identical factor is required and it becomes irrelevant for the linearity of the (weighted) least squares equations. Hence we can attempt to use directly the amplitude of histogram as ("dirty") effective  $\sigma$  and observe the effects in the fit. The "lucky" results are illustrated in fig. 6 for this "dirty-lucky" model. This figure is produced as fig. 4 with the sole difference given by the use of the "dirty" effective  $\sigma$  in the weighted least squares.

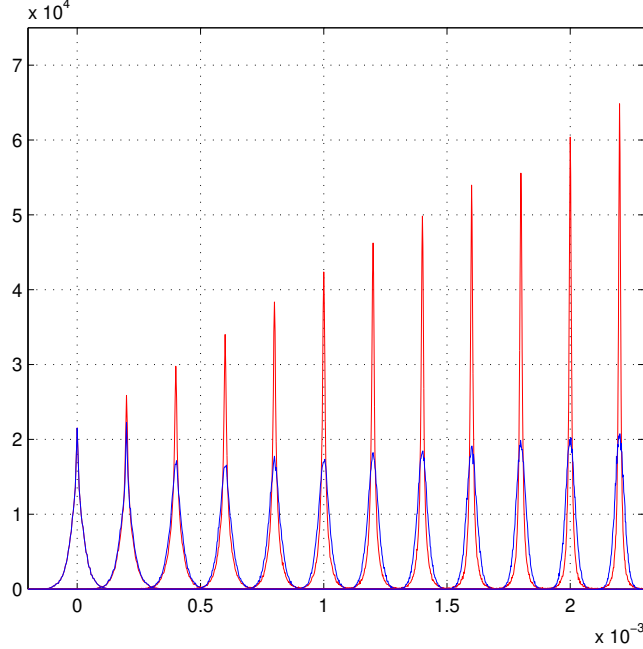


Figure 6: The dirty (lucky) model. The blue distributions are the standard least squares. The red distributions are the  $\gamma_f$  given by the dirty-lucky-model, very near to those of the schematic model.

The maximum of fig. 6 is around  $6.5 \cdot 10^4$  and fig. 4 is around  $7.2 \cdot 10^4$ : the results of the fits are excellent. The robustness of the heteroscedasticity is evident. Large variations of the details of the parameters (probability distributions) of the models do not modify the fit results. For example, the use of the effective variances, illustrated with the red line in fig. 1, with the  $\eta$ -positioning gives  $\gamma_f$ -distributions identical to the complete schematic model. This result is easy to justify, the weights inserted in the least squares are  $\sigma^{-2}$ , and the higher  $\sigma$ -values are all compressed near to zero, and their differences compared to the constant value of fig. 1 become negligible. Instead, the lower  $\sigma$ -values are very similar in the two models and they dominate the fits. We even test the "dirty"  $\sigma$  approximation with the three strip COG (COG<sub>3</sub>) histogram and its corresponding  $\eta$  positioning ( $\eta_3$ ). Even here, the linear growth is clearly evident but the maximum is around 1/2 of that of fig. 4. The strip added to the COG<sub>2</sub>, to compose the COG<sub>3</sub>, is almost always pure noise at this orthogonal incidence [8]. In addition, the COG<sub>3</sub> has discontinuities at the strip borders [7], here very small and masked by the noise, but just in the region with the best  $\sigma$ . Thus this lower result is not unexpected, and it is consistent with our full three strips schematic model. Similar tests were performed on the low noise floating strip side.

## 5 Hints for an experimental verification

Some of the results presented here could be verified with a test beam. The beam divergence should be less than  $10^{-5}$  radians, probably not easy to obtain. In the simulations we used a very simplified (for the computer) approach: the detector-layer configurations were generated each time dividing symmetrically the allowed interval from the first and last layer. This correspond to a different experimental set up for

any layer number. A more realistic set up could be composed with a fixed number of parallel detector layers, (normal silicon micro-strips) orthogonal to the beam (of high momentum to limit the multiple scattering). An effective increase of the layer number can be produced varying those inserted in the fit. Excellent precisions in the tracker alinement and of the beam divergence are required. The  $\eta$  algorithm is essential. At orthogonal incidence and without magnetic field the  $\eta$ -corrections are very small or negligible. In any case for parallel tracks the corrections are identical and their neglect implies a parallel translation of the tracks. The  $\chi^2$  and the dirty-lucky model can be used to test heteroscedasticity.

If the beam divergence is large compared to the  $\gamma_f$  resolution of the fit, the presence of the linear growth can be observed in the fluctuation of the difference of the  $\gamma_f$  fitted with all the available layers and the  $\gamma_f$  fitted with the elimination of a layer each time in the same track. The linear growth produces a parabolic increase of these differences. The standard fit produces a small increase in the last couple of differences.

## 6 Conclusions

Simple simulations produce linear growths in the fit resolution, similar to those of ref. [2] for the momentum reconstruction. Here, straight tracks of a well collimated beam are used and the direction  $\gamma$  of the track is the test parameter. This two parameter fit is easier than that for the momentum. The gaussian model easily produces the linear growth of the fit resolution. The model is so simple, for its essential mathematics, that it can completed with a few lines of MATLAB code and its results are almost identical to our very complicated schematic model. The addition of the physics of the detectors is a heavy task. The evident similarity of the effective  $\sigma$  scatter-plots with the histograms of the two strips center of gravity triggered a more accurate analysis of its origin. This analysis was sufficiently convincing to try a weighted least squares fit with weights extracted from the center of gravity histogram (the dirty-lucky model). The result of this test is excellent with a drastic increase of the fit resolution and the sought linear growth. The differences of the dirty-lucky model compared to the schematic model are around 10 %, a negligible price compared to the enormous simplification in the the extraction of the weight. It is evident that these are very preliminary results, and further tests are essential before a systematic use of the model. Very synthetic indications are given for a experimental verification of the model.

## Acknowledgments

Many tanks are due to Prof. A. Baracca, physicist and historian of physics, for his suggestion to look for and where to find the original Gauss papers on least squares. The Gauss papers were very stimulating for our work.

## References

- [1] G. Landi, G.E. Landi, *Improvement of track reconstruction with well tuned probability distributions* JINST 9 2014 P10006. arXiv:1404.1968[physics.ins-det] <https://arxiv.org/abs/1404.1968>
- [2] G. Landi, G.E. Landi *Optimizing momentum resolution with a new fitting method for silicon-strip detectors* INSTRUMENTS **2018**, 2, 22 arXiv:1806.07874[physics.ins-det] <https://arxiv.org/abs/1806.07874>
- [3] F. Hartmann. *Silicon tracking detectors in high energy physics*. Nucl. Instrum. and Meth. A 666 (2012) 25



- [4] MATLAB 8. The MathWorks Inc.
- [5] K.A. Olive et al. *Particle Data Book* Chin. Phys. C **38** 090001 (2014)
- [6] E. Belau, R. Klanner, G. Lutz, E. Neugebauer, H. J. Seebrunner, A. Wylie, *Charge collection in silicon strip detector* [http://dx.doi.org/10.1016/0167-5087\(83\)90591-4](http://dx.doi.org/10.1016/0167-5087(83)90591-4) *Nucl. Instrum. and Meth. A* 214 (1983) 253.
- [7] G. Landi, *Properties of the center of gravity as an algorithm for position measurements* [http://dx.doi.org/10.1016/S0168-9002\(01\)02071-X](http://dx.doi.org/10.1016/S0168-9002(01)02071-X) *Nucl. Instrum. and Meth. A* 485 (2002) 698.
- [8] G. Landi, *Problems of position reconstruction in silicon microstrip detectors*, <http://dx.doi.org/10.1016/j.nima.2005.08.094> *Nucl. Instr. and Meth. A* 554 (2005) 226.
- [9] G. Landi and G.E. Landi, *"Asymmetries in Silicon Microstrip Response Function and Lorentz Angle"* arXiv:1403.4273[physics.ins-det] <http://arxiv.org/abs/1403.4273>
- [10] O. Adriani et al., *"In-flight performance of the PAMELA magnetic spectrometer"* 16<sup>th</sup> *International Workshop on Vertex Detectors* September 2007 NY. USA. PoS(Vertex 2007)048